Linear and nonlinear characteristics of time-resolved photoluminescence modulation by terahertz pulse*

Jiao-Li Gong(龚姣丽)[1,2], Jin-Song Liu(刘劲松)[1,†], Man Zhang(张曼)[1], Zheng Chu(褚政)[1], Zhen-Gang Yang(杨振刚)[1], Ke-Jia Wang(王可嘉)[1], and Jian-Quan Yao(姚建铨)[1]

[1] *Wuhan National Laboratory for Optoelectronics, School of Optical and Electronic Information, Huazhong University of Science and Technology, Wuhan* 430074, *China*

[2] *Hubei Collaborative Innovation Center for High-efficient Utilization of Solar Energy, School of Science, Hubei University of Technology, Wuhan* 430068, *China*

(Received 10 April 2017; revised manuscript received 10 May 2017; published online 20 August 2017)

The linear and nonlinear characteristics of time-resolved photoluminescence (PL) of n-type bulk semiconductor GaAs modulated with terahertz (THz) pulse are studied by using an ensemble Monte Carlo (EMC) method. In this paper the center energy valley (Γ valley) electron concentration changes with the pulse delay time, sampling time and the outfield are mainly discussed. The results show that the sampling time and the THz field should exceed certain thresholds to effectively excite photoluminescence quenching (PLQ). Adopting a direct current (DC) field makes the sampling time threshold shortened and the linear range of THz field-modulation PL expanded. Moreover, controlling the sampling time and the outfield intensity can improve the linear quality: with forward time, the larger outfield is used; with backward time, the smaller outfield is used. This study can provide a theoretical basis of THz field linear modulation in a larger range for new light emitting devices.

Keywords: THz pulse modulation, photoluminescence, ensemble Monte Carlo, intervalley scattering

PACS: 02.50.Ng, 42.65.Re, 42.65.Sf, 71.55.Eq **DOI:** 10.1088/1674-1056/26/10/100201

1. Introduction

THz pulse based on its high-field transport and ultrafast characteristics has been applied to semiconductor modulation technology which has seen rapid development in recent years.[1–12] Especially, it is possible to study the nonlinear modulation of the carriers by THz pulse precision delay in semiconductors. For example, scholars have observed nonlinear ultrafast modulations of intense terahertz pulses in Ge, Si, GaAs, and InGaAs.[5,6] Su *et al*. studied the ultrafast dynamics of GaAs photoexcited carriers in THz field.[7] The nonlinear phenomenon about impact ionization and intervalley scattering are observed in InSb and InAs with intense terahertz pulses.[8–10]

As a way of reflecting the interaction between THz pulse and electrons, photoluminescence (PL) has attracted wide attention.[13–19] For instance, the THz-induced photoluminescence quenching phenomenon is observed by using the terahertz wave as a quenching source and the femtosecond laser with a wavelength of 800 nm as an excitation source.[14,19] Liu *et al*. in 2010 observed the PLQ phenomenon of CdTe and GaAs from single-cycle THz pulse by using the time-integrated PL spectra measurement.[15] In 2011, Bhattacharyya *et al*. reported that the free electron laser is used to study the time-resolved PLQ effect of semiconductor quantum wells,[16] and the magnetoexcitonic photoluminescences from GaAs/AlGaAs quantum wells were realized by time-resolved terahertz quenching in 2014.[17]

From the previous studies, we learn THz coherent detection based on time-resolved PL[19] in bulk semiconductor, and the PL intensity $I_{\rm PL}$ shows some nonlinear characteristics with the change of THz field $E_{\rm THz}$. However, from the view of THz field-modulation PL and measurement, it is hoped that $I_{\rm PL}$ changes with $E_{\rm THz}$ linearly, whose range needs expanding as much as possible. To solve the problems, further research has been performed. We select bulk material GaAs with lower n-doping density ($n = 10^{16}/{\rm cm}^3$) for numerically analyzing the influence of THz wave on semiconductor carriers by using the ensemble Monte Carlo method.[19–23] Furthermore, in this work, the relationship between time-resolved PL intensity and THz pulse is studied (see Fig. 1). With the understanding of nonlinear characteristics, we study how to control PL sampling time and direct current (DC) field to realize the linear change, whose range can be determined and expanded. This study can provide the theoretical basis of THz field linear modulation in a larger range for new light emitting devices.

2. Physical model

In the process of optical excitation-THz modulation, Boltzmann equations are used to describe the carrier–phonon

*Project supported by the National Natural Science Foundation of China (Grant Nos. 11574105, 61475054, 61405063, and 61177095), the Hubei Science and Technology Agency Project, China (Grant No. 2015BCE052), and the Fundamental Research Funds for the Central Universities, China (Grant No. 2017KFYXJJ029).

†Corresponding author. E-mail: jsliu4508@vip.sina.com

© 2017 Chinese Physical Society and IOP Publishing Ltd

system as follows:[19–22]

$$\frac{\partial f_k}{\partial t} = \left.\frac{\partial f_k}{\partial t}\right|_{\rm g} + \left.\frac{\partial f_k}{\partial t}\right|_{\rm c-ph} + \left.\frac{\partial f_k}{\partial t}\right|_{\rm c-impurity} + \frac{eE_t(t)}{\hbar}\nabla_k f_k, \quad (1)$$

$$\frac{\partial N_q}{\partial t} = \left.\frac{\partial N_q}{\partial t}\right|_{\rm c-ph} + \left.\frac{\partial N_q}{\partial t}\right|_{\rm ph-ph}, \quad (2)$$

f_k and N_q are the distribution functions of electrons and phonons, respectively; $\partial f_k/\partial t|_{\rm g}$ is the optical excitation probability; $\partial f_k/\partial t|_{\rm c-ph}$ and $\partial f_k/\partial t|_{\rm c-impurity}$ are the probabilities of carrier–phonon and carrier–impurity scattering, respectively; $\partial N_q/\partial t|_{\rm c-ph}$ and $\partial N_q/\partial t|_{\rm ph-ph}$ carrier–phonon and phonon–phonon interaction rates, respectively; $eE_t(t)\nabla_k f_k/\hbar$ describes the process of THz-field-drive carriers, e is the elementary charge, $\hbar$ the Planck constant, and E_t the THz field transmitted through the semiconductor.[7] We use the ensemble Monte Carlo method to simulate the dynamics of carriers in the study.[23] A three-alley model (Γ–L–X) is used to describe the nonparabolic conduction band structure. The carrier–phonon scattering rate mainly includes acoustic phonon scattering, intervalley scattering, intravalley scattering, polar optical phonon scattering, etc.

The parameters[19,24,25] used for calculation are as follows: laser wavelength $\lambda = 800$ nm; laser photon energy $E = 1.54$ eV; laser pulse width $w_0 = 40$ fs; bulk GaAs size: 1 mm×1 mm; GaAs band gap $E_{\rm g} = 1.42$ eV; intervalley energy $E_{\Gamma L} = 0.29$ eV, $E_{\Gamma X} = 0.52$ eV; effective mass $m_\Gamma/m_0 = 0.067$, $m_L/m_0 = 0.22$, $m_X/m_0 = 0.58$, $m_{hh}/m_0 = 0.45$; lattice temperature: $T_{\rm Lattice} = 300$ K; phonon energy (eV): $\hbar\omega_{\rm LO} = 0.035$, $\hbar\omega_{\Gamma L} = 0.0278$, $\hbar\omega_{\Gamma X} = 0.0299$, $\hbar\omega_{LX} = 0.0293$, $\hbar\omega_{LL} = 0.0290$, $\hbar\omega_{XX} = 0.0299$; sound velocity $v_{\rm s} = 5.24$ km/s; lattice density $\rho = 5.36$ g/cm^3; lattice constant $a_0 = 5.64$ Å; static dielectric function $\varepsilon_0 = 12.9$; and high-frequency dielectric function $\varepsilon_\infty = 10.9$.

3. Results and discussion

The laser pulse with a wavelength of 800 nm can effectively excite electrons from the valence band to the bottom of the conduction band. As the photon energy and GaAs band gap are close, the excited free carrier energy is very low. In the absence of THz pulse, the matching conditions of the wave vector are satisfied with the recombination of the electrons at the bottom of the conduction band Γ valley and the holes in the valence band. It has fast recombination luminescence without the participation of the phonons, thus forming PL. Under the intense THz field, free carriers will be accelerated thus transferred to a high-energy satellite valley outside the Γ valley (the intervalley scattering). Those electrons cannot be directly recombined with holes in the valence band, resulting in weakening PL and forming PLQ (See Fig. 1).

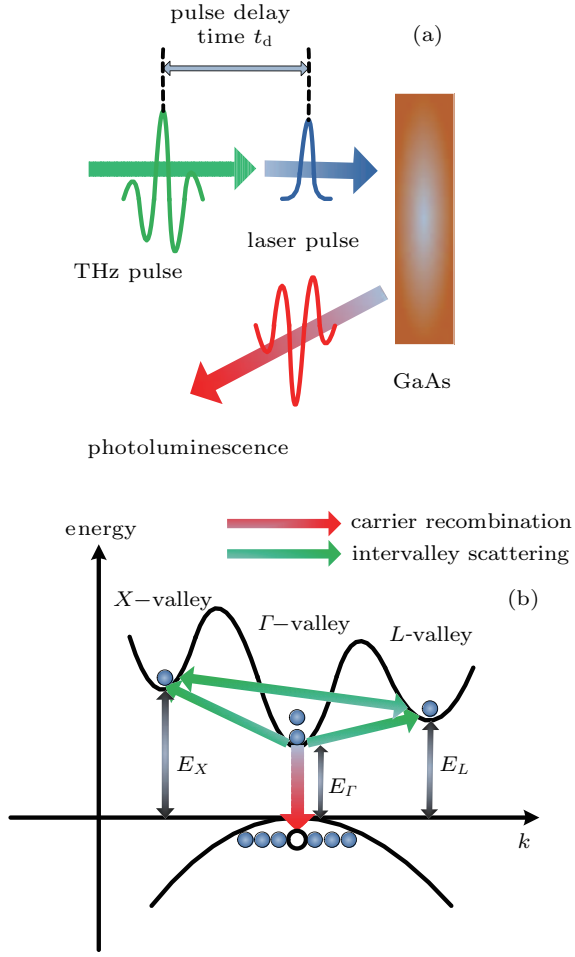


Fig. 1. (color online) (a) Photoluminescence modulation by THz pulse in n-type bulk GaAs at room temperature. (b) Physical mechanism for the PL-modulation. The red arrow denotes the recombination of the electrons in the conduction band Γ valley and the holes in the valence band, and thus forming PL. Green arrows refer to the intervalley scattering mechanism that causes the electrons to transfer from the Γ valley to the L and X valleys.

In the time domain, the time-resolved PL intensity $I_{\rm PL}$ is proportional to the electron density of the Γ valley,[26,27] the variation of electron distribution in each valley can be obtained through solving the distribution Eqs. (1) and (2) by the EMC method. The electron density change in the Γ valley can be defined as

$$P = 100\% \times \frac{n_\Gamma({\rm THz} \neq 0)}{n_\Gamma({\rm THz} = 0)}, \quad (3)$$

where $n_\Gamma({\rm THz} \neq 0)$ and $n_\Gamma({\rm THz} = 0)$ are the electron density of the Γ valley in the presence and absence of a THz field, respectively. So the PL intensity $I_{\rm PL} \propto P$, the decrease proportion of electron concentration in the Γ valley is $Q = 1 - P$, and then, the PLQ intensity $I_{\rm PLQ} \propto Q$.

Therefore, we can investigate the changes of time-resolved PL by studying the P value. The linear and nonlinear variation characteristics of PL can be studied through the changes of P value with pulse delay time $t_{\rm d}$, sampling time t, THz field $E_{\rm THz}$, and DC field $E_{\rm DC}$. Here, $t_{\rm d}$ is the relative delay time between THz pluse and pump laser pulse, and $t_{\rm d} > 0$

means that the THz pulse precedes the peak of the laser pulse; t is the PL sampling time. The dynamic evolutions of carriers can be described by changing t_d and t.

3.1. PL modulation by THz pulse without DC field

First of all, we analyze the results of PL by directly modulating the THz field without a DC field. Figure 2(a) shows the incident THz field, with a center frequency of 1.1 THz. Figure 2(b) shows that the THz peak intensity is fixed to 100 kV/cm without the DC field. It can be found at different sampling time t, P value of electron density in Γ valley changes with pulse delay time t_d. When the THz pulse peak coincides with the laser pulse peak ($t_d = 0$), P is minimum, namely Q reaches a maximum value.

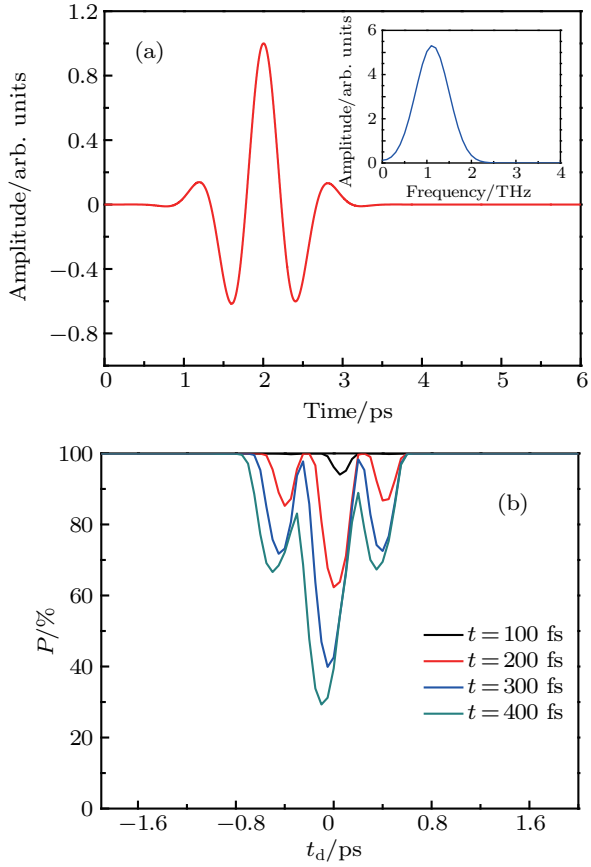


Fig. 2. (color online) (a) The incident THz pulse of the time–domain spectrum and the frequency spectrum (the inset) with center frequency of 1.1 THz. (b) $E_{DC} = 0$, $E_{THz} = 100$ kV/cm, the P value changes with pulse delay time t_d.

We can observe two phenomena. Firstly, the reduction of electron density corresponds to the intervalley scattering and PLQ. The P value is sensitive to the THz field intensity: the stronger strength of the THz field means that the P value is weakened more greatly, namely the intervalley scattering and PLQ rate are greater. Thus, the information about THz intensity can be well understood through the P value. However, there is no response for THz transient polarization direction, and the P value can only provide amplitude information no matter whether the drive pulse is positive or negative.

Secondly, the P value is different at different sampling time t. When $t = 100$ fs, P is relatively large, indicating that at the beginning of time, there are a small number of electrons involved in intervalley scattering. When $t = 200$ fs, the minimum of P is about 62%, with good linear effect. At 400 fs, the P value can reach 30%, but with the strengthened nonlinear characteristics. There is a certain distortion of P-value shape, as it is unable to respond well to THz intensity changes. In general, when t is relatively small, the PL shows a linear change with the THz intensity; when t is relatively large, the PL shows a nonlinear change.

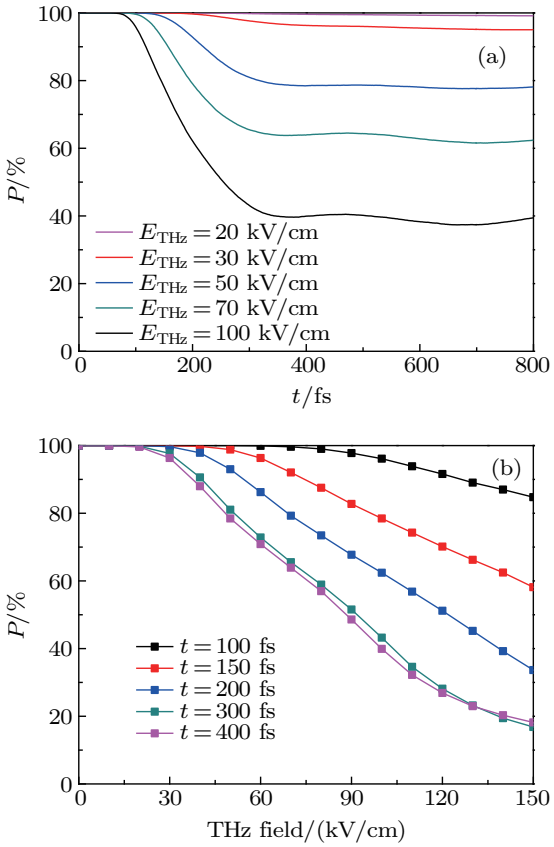


Fig. 3. (color online) (a) Peaks of Q changing with t under the different THz fields, $E_{DC} = 0$, $t_d = 0$. (b) Peaks of Q changing with THz fields at different values of sampling time t.

In order to understand the variation regulation of the P value at different values of sampling time t, t_d is fixed to be 0. Figure 3(a) shows that the peaks of Q (the lowest point of P) change with t under the different THz fields. At the beginning, the energy of electrons is not sufficient to cause the intervally scattering. With the unchanged number of electrons in the Γ valley, the P value is 100%. After the time threshold, the P value decreases almost linearly, tending to be saturated after reaching the lowest point. The smaller THz field intensity results in the longer time to reach the threshold as well as the smaller linear range. When $E_{THz} = 100$ kV/cm, it has a better linear relationship between 100 fs and 300 fs. If more than 300 fs, the electronic energy is gradually accumulated over time, in addition to the Γ–L valley scattering, the Γ–X

valley scattering and the *L*–*X* scattering also occur. It leads to nonuniform energy absorption, gradually-saturated scattering and a little-changed *P* value. Comparing with Fig. 2(b) shows that the shape of *P* changes largely when $t > 300$ fs, no longer with a significant linear relationship with THz waveform.

Figure 3(b) shows that the *Q* peak changes with THz field without DC field. We select and study the THz fields at 0 kV/cm–150 kV/cm (peak value). Firstly, THz intensity should exceed a certain threshold to effectively accelerate electrons, thus forming intervally scattering and photoluminescence quenching. Secondly, at different values of sampling time *t*, the thresholds to be exceeded are different. For instance, when $t = 150$ fs, intervally scattering occurs after 40 kV/cm, showing a good linear relationship after 50 kV/cm. That is, the *Q* value increases linearly with THz field intensity. However, with time going by, the intervally scattering is gradually saturated, with the reduced linear quality and the narrowed linear range, e.g., when $t = 300$ fs, it has a relatively good linear relationship only at 30 kV/cm–120 kV/cm.

3.2. PL modulation by THz pulse with DC field

Based on the above analysis, we find that the sampling time and the THz field should exceed their certain thresholds to effectively excite PLQ. Adopting a DC field can make the sampling time threshold shortened and the linear range of THz field-modulation PL expanded. Here we analyze the changes of *P* value with pulse delay time t_d under the DC and THz fields. It is supposed that DC field $E_{DC} = 30$ kV/cm, and $t = 300$ fs (See Fig. 4(a)). Firstly, with the increase of THz peak value, *Q* peak position declines. While when THz field approaches 0, the equilibrium position of *P* is 95%, only with the function of DC field. It indicates that the DC field can provide electrons with stable and enduring energy to keep them in the active scattering states, thus overcoming the influence of the threshold effect on the PL response. Secondly, the introduction of the DC field causes the carriers to form directional transport, and the change of external THz field direction leads to the change of carrier transport velocity. In this way, the *P* value can provide the vibration direction of THz pulse.

Figure 4(b) shows the result from changing *t* by DC field $E_{DC} = 30$ kV/cm and THz field (peak value) $E_{THz} = 20$ kV/cm. It indicates that the shape of *P* is modulated by the THz field, and the equilibrium position of *P* in the figure is controlled by the DC field. The degree of quenching by DC field has a direct relationship with time *t*. As *t* passes, overall, the *P* value moves downward. Therefore, it can improve the linear quality of THz field response by controlling *t*, and search for a larger linear THz field modulation range.

In the above example, we select the smaller outfield ($E_{DC} + E_{THz}$) (see Fig. 4(b)) and backward sampling time *t* (see Fig. 4(a)). Specific reasons can be analyzed from Fig. 5.

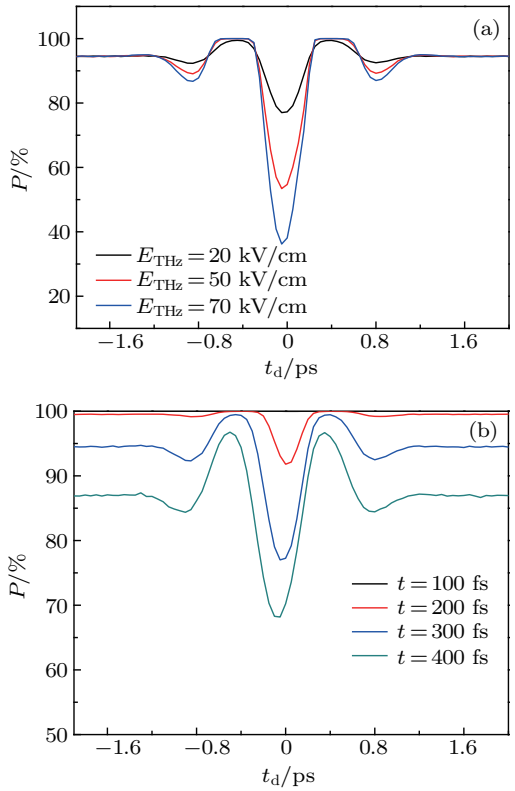


Fig. 4. (color online) (a) *P* values changing with pulse delay time t_d in different THz fields, at $E_{DC} = 30$ kV/cm and $t = 300$ fs. (b) *P* values changing with pulse delay time t_d at different values of sampling time *t*, $E_{DC} = 30$ kV/cm and $E_{THz} = 20$ kV/cm.

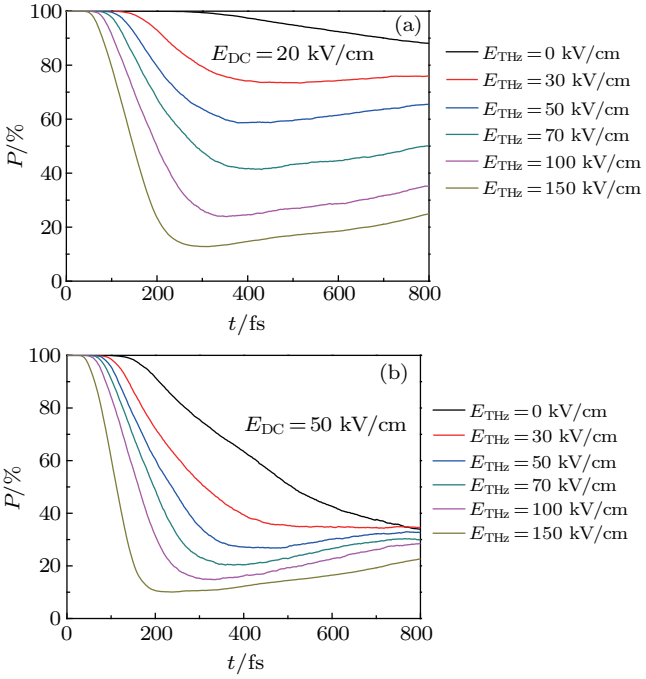


Fig. 5. (color online) Variations of *Q* peak value with sampling time *t* in different THz fields and DC fields: (a) DC field $E_{DC} = 20$ kV/cm and (b) DC field $E_{DC} = 50$ kV/cm.

When $t_d = 0$, the *P* value is minimum and the *Q* value is maximum. Figure 5 shows the changes of *Q* peak value with sampling time *t* in different DC fields and THz fields.

These changes are different for the linear range, generally, in the time range of 50 fs–400 fs. Unlike figure 3(a), with the increased DC field and relatively small THz field, the time for exceeding the threshold is shortened, and the linear time range is expanded; when the THz field is relatively large, the P value speeds up the decrease with increasing DC field, the PLQ accelerates formation and the linear time range is narrowed down.

In addition, when the time is relatively forward, it needs a larger outfield to overcome the threshold of intervally scattering for good linear modulation; when the time is backward, the carriers accumulate enough energy, thus being prone to causing a nonlinear effect. Then, the smaller outfield can obtain good linear modulation. According to the above results and their analyses, we can select the appropriate sampling time t and outfield.

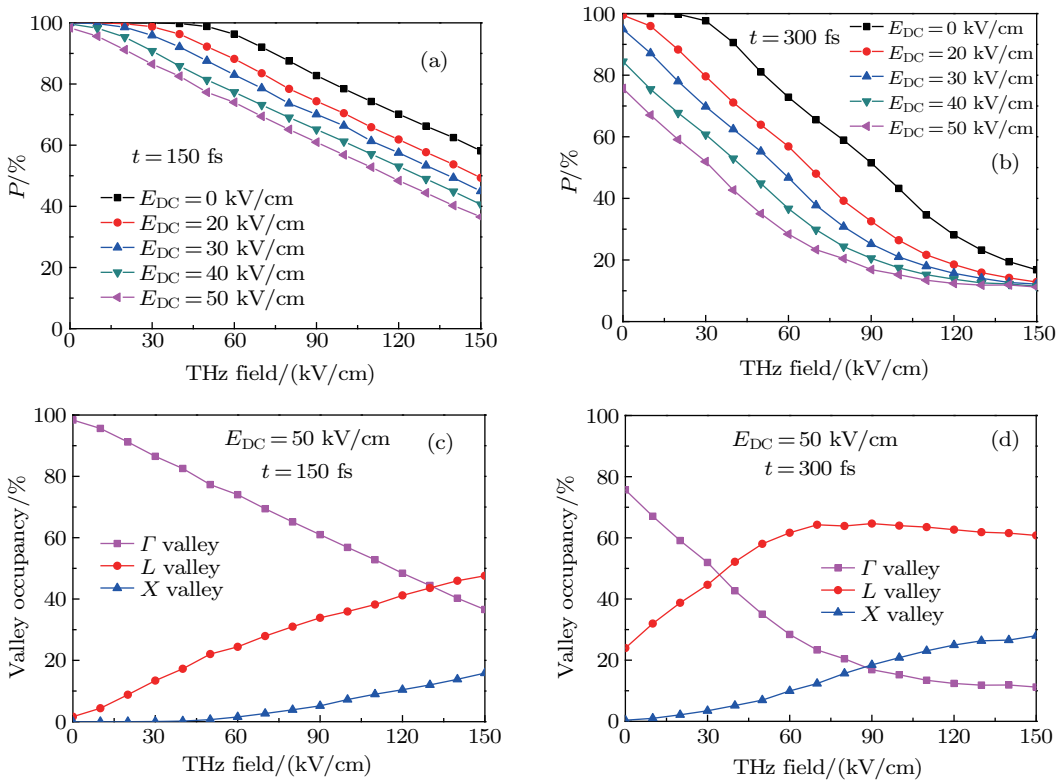


Fig. 6. (color online) Variations of peak of Q changes with THz fields in different DC fields at (a) $t = 150$ fs and (b) $t = 300$ fs. Three valley occupancies varying with THz field at DC field $E_{DC} = 50$ kV/cm, and (c) $t = 150$ fs and (d) $t = 300f$ s, respectively.

According to Figs. 5(a) and 5(b), we select two time points for comparison. Figures 6(a) and 6(b) show the peaks of Q change with THz fields in different DC fields at $t = 150$ fs and $t = 300$ fs, respectively. In these figures the horizontal axes are both THz field intensity. It can be found that the THz field linear range is 50 kV/cm–150 kV/cm at 150 fs without DC field. When DC field is 50 kV/cm, it can directly exceed threshold, so that THz field can be linearly modulated in the range of 0 kV/cm–150 kV/cm. As to the case without a DC field, the linear range is significantly expanded. When the DC electric field continues to increase, the P value decreases with PLQ deepening and starting position declining.

When $t = 300$ fs, the electrons accumulate enough energy, with obvious nonlinearity. When the outfield is high to a certain extent ($E_{DC} + E_{THz} > 120$ kV/cm), the quenching tends to be saturated, no longer having a linear relationship with THz field. With the increase of DC field, the THz field linear modulation range is gradually reduced to the low field direction, and the best value is obtained with a DC field of about 30 kV/cm.

In order to further illustrate different linearities at different time points, we study the electron percentage occupancies in three valleys when $E_{DC} = 50$ kV/cm (the purple curve in Figs. 6(a) and 6(b)). Figure 6(c) shows that when the DC field is 50 kV/cm and $t = 150$ fs, the electrons in L and X valleys account for a certain proportion in a manner similar to linear growth. Then, the electron proportion of Γ valley is linear. Compared with the scenario in Fig. 3(b), on the one hand, the DC field here exceeds the electric field threshold; on the other hand, high-energy electrons cause Γ–X and L–X scatterings. Due to the forward sampling time, the energy absorptions are relatively uniform for these two scattering mechanisms, resulting in the expansion of the linear range of PLQ to THz intensity. Figure 6(d) shows that when DC field $E_{DC} = 50$ kV/cm, and $t = 300$ fs, the linear regions of L and X valleys do not synchronize at this time point, exhibiting obvious nonlinear characteristics. Especially when the THz field exceeds 70 kV/cm, the electrons of L valley tend to be saturated, resulting in the electrons of Γ valley varying with a nonlinear trend.

4. Conclusions

We study the linear and nonlinear characteristics of time-resolved PL of n-type bulk semiconductor GaAs modulated by THz pulse by using the EMC method. The results show that there are two ways to improve PLQ linear quality and range: controlling the sampling time t and controlling the outfield ($E_{\mathrm{DC}} + E_{\mathrm{THz}}$). Specifically, (i) the sampling time and the THz field intensity should exceed their certain thresholds to effectively excite electrons for intervalley scattering, thus producing PLQ. (ii) Adopting the DC field can make the time threshold shortened and the linear range of THz field modulation PL expanded. (iii) Controlling the sampling time and the outfield intensity as well as improving the linear quality: in a forward sampling time, the outfield need to exceed its large threshold. The energy absorption is relatively uniform for each of Γ–L, Γ–X and L–X scatterings. Thus, we should use the larger outfield. In a backward sampling time, electron energy accumulation behaves nonlinearly, and the linear regions of Γ, L, and X valleys do not synchronize. Thus, we should use the smaller outfield. Future simulations can be considered to study the time-resolved PL and PLQ dependence on THz frequency, temperature, optical-excitation intensity, semiconductors with different materials, etc. These studies will provide the theoretical basis for the light emitting units of new THz field modulation.

References

[1] Hughes S and Citrin D S 1998 *Phys. Rev. B* **58** R15969
[2] Gaal P, Kuehn W, Reimann K, Woerner M, Elsaesser T, Hey R, Lee J S and Schade U 2008 *Phys. Rev. B* **77** 235204
[3] Hirori H, Nagai M and Tanaka K 2010 *Phys. Rev. B* **81** 081305
[4] Hoffmann M C, Monozon B S, Livshits D, Rafailov E U and Turchinovich D 2010 *Appl. Phys. Lett.* **97** 231108
[5] Hebling J, Hoffmann M C, Hwang H Y, Yeh K L and Nelson K A 2010 *Phys. Rev. B* **81** 035201
[6] Razzari L, Su F H, Sharma G, Blanchard F, Ayesheshim A, Bandulet H C, Morandotti R, Kieffer J C, Ozaki T, Reid M and Hegmann F A 2009 *Phys. Rev. B* **79** 193204
[7] Su F H, Blanchard F, Sharma G, Razzari L, Ayesheshim A, Cocker T L, Titova L V, Ozaki T, Kieffer J C, Morandotti R, Reid M and Hegmann F A 2009 *Opt. Express* **17** 9620
[8] Wen H, Wiczer M and Lindenberg A M 2008 *Phys. Rev. B* **78** 125203
[9] Hoffmann M C, Hebling J, Hwang H Y, Yeh K L and Nelson K A 2009 *Phys. Rev. B* **79** 161201
[10] Ho I C and Zhang X C 2011 *Appl. Phys. Lett.* **98** 241908
[11] Du L L, Li Q, Li S X, Hu F R, Xiong X M, Li Y F, Zhang W T and Han J G 2016 *Chin. Phys. B* **25** 027301
[12] Zhou W, Ji K and Chen H M 2017 *Acta Phys. Sin.* **66** 054210 (in Chinese)
[13] Quinlan S M, Nikroo A and Sherwin M S 1992 *Phys. Rev. B* **45** 9428
[14] Zybell S, Schneider H, Winnerl S, Wagner M, Kohler K and Helm M 2011 *Appl. Phys. Lett.* **99** 041103
[15] Liu J, Kaur G and Zhang X C 2010 *Appl. Phys. Lett.* **97** 111103
[16] Bhattacharyya J, Wagner M, Zybell S, Winnerl S, Stehr D, Helm M and Schneider H 2011 *Rev. Sci. Instrum.* **82** 103107
[17] Bhattacharyya J, Zybell S, Esser F, Helm M, Schneider H, Schneebeli L, Bottge C N, Breddermann B, Kira M and Koch S W 2014 *Phys. Rev. B* **89** 125313
[18] Zybell S, Bhattacharyya J, Winnerl S, Esser F, Helm M, Schneider H, Schneebeli L, Bottge C N, Kira M and Koch, S W 2014 *Appl. Phys. Lett.* **105** 201109
[19] Chu Z, Liu J and Wang K 2012 *Opt. Lett.* **37** 1433
[20] Jacoboni C and Reggiani L 1983 *Rev. Mod. Phys.* **55** 645
[21] Lugli P, Bordone P, Reggiani L, Rieger M, Kocevar P and Goodnick S M 1989 *Phys. Rev. B* **39** 7852
[22] Collins C L and Yu P Y 1983 *Phys. Rev. B* **27** 2602
[23] Gong J L, Liu J S, Chu Z, Yang Z G, Wang K J and Yao J Q 2016 *Chin. Phys. B* **25** 100203
[24] Fischetti M V 1991 *IEEE Trans. Electron Dev.* **38** 634
[25] Johnston M B, Whittaker D M, Corchia A, Davies A G and Linfield E 2002 *Phys. Rev. B* **65** 165301
[26] Shah J, Deveaud B, Damen T C, Tsang W T, Cossard A C and Lugli P 1987 *Phys. Rev. Lett.* **59** 2222
[27] Elsaesser T, Shah J, Rota L and Lugli P 1991 *Phys. Rev. Lett.* **66** 1757